MOLECULAR AND CELLULAR BIOLOGY, Feb. 2005, p. 1025–1040 Vol. 25, No. 3
0270-7306/05/$08.00+0 doi:10.1128/MCB.25.3.1025–1040.2005

Inhibition of Macroautophagy Triggers Apoptosis†

Patricia Boya,[1]‡§ Rosa-Ana González-Polo,[1]‡ Noelia Casares,[1] Jean-Luc Perfettini,[1] Philippe Dessen,[1] Nathanael Larochette,[1] Didier Métivier,[1] Daniel Meley,[2] Sylvie Souquere,[3] Tamotsu Yoshimori,[4] Gérard Pierron,[3] Patrice Codogno,[2] and Guido Kroemer[1]*

CNRS-UMR8125, Institut Gustave Roussy,[1] and Laboratoire Replication de l'ADN et Ultrastructure du Noyau, UPR-1983,[3] and INSERM U504,[2] Institut André Lwoff, Villejuif, France, and National Institute of Genetics, Mishima, Japan[4]

Received 6 May 2004/Returned for modification 8 June 2004/Accepted 19 October 2004

Mammalian cells were observed to die under conditions in which nutrients were depleted and, simultaneously, macroautophagy was inhibited either genetically (by a small interfering RNA targeting *Atg5*, *Atg6*/*Beclin 1-1*, *Atg10*, or *Atg12*) or pharmacologically (by 3-methyladenine, hydroxychloroquine, bafilomycin A1, or monensin). Cell death occurred through apoptosis (type 1 cell death), since it was reduced by stabilization of mitochondrial membranes (with *Bcl-2* or *vMIA*, a cytomegalovirus-derived gene) or by caspase inhibition. Under conditions in which the fusion between lysosomes and autophagosomes was inhibited, the formation of autophagic vacuoles was enhanced at a preapoptotic stage, as indicated by accumulation of LC3-II protein, ultrastructural studies, and an increase in the acidic vacuolar compartment. Cells exhibiting a morphology reminiscent of (autophagic) type 2 cell death, however, recovered, and only cells with a disrupted mitochondrial transmembrane potential were beyond the point of no return and inexorably died even under optimal culture conditions. All together, these data indicate that autophagy may be cytoprotective, at least under conditions of nutrient depletion, and point to an important cross talk between type 1 and type 2 cell death pathways.

Type 1 (apoptotic) cell death and type 2 (autophagic) cell death are viewed as clearly distinct subroutines of cellular demise (9, 42, 47). Apoptosis, which is currently viewed as the quantitatively most important death modality, is morphologically defined by cellular and nuclear shrinkage (pyknosis), chromatin condensation, blebbing, nuclear fragmentation (karyorrhexis), and formation of apoptotic bodies (32). At the biochemical level, apoptosis of mammalian cells is characterized by mitochondrial membrane permeabilization (MMP) and/or massive caspase activation (1, 21, 68). Autophagic cell death is characterized by the accumulation of autophagic vacuoles (AV) (see below). Although less frequent, type 2 cell death is pathophysiologically relevant. For example, type 2 cell death affects degenerating neurons in some pathologies (17, 39), participates in retinal degeneration (24), seals the fate of *Salmonella*-infected macrophages (26), and sometimes mediates chemotherapy-induced tumor killing (30, 31, 55). Moreover, an important autophagy-regulatory gene such as *Beclin 1* functions as a haploinsufficient tumor suppressor gene (60, 76), further underscoring the likely clinical importance of type 2 cell death. Nonetheless, the biochemical mechanisms accounting for cell killing remain largely unexplored in type 2 cell death, and the mutual relationship between apoptotic and autophagic death is currently debated (20, 27, 41–43, 48, 62, 70, 72, 75).

Autophagy is a regulated process of degradation and recycling of cellular constituents, participating in organelle turnover and in the bioenergetic management of starvation (37). During autophagy, part of the cytoplasm or entire organelles are sequestered into double-membraned vesicles, called AV or autophagosomes. Autophagosomes ultimately fuse with lysosomes, thereby generating single-membraned autophagolysosomes and degrading their content (73). Autophagy has been extensively studied in *Saccharomyces cerevisiae*, especially at the genetic level, leading to the discovery of autophagy-relevant *Apg* and *Aut* genes, now renamed *Atg* genes (36, 61). Several Atg proteins have been implicated in autophagosome formation. The ubiquitinization of Atg5 and Atg12 by the E1-like enzymes Atg7 and Atg10 is required to recruit other proteins to the autophagosomal membrane and to form the autophagic vacuole in a pathway, which was first elucidated for yeast and then confirmed for mammalian cells (51, 53). LC3 is the mammalian equivalent of yeast Atg8. It exists in two forms, LC3-I and its proteolytic derivative LC3-II (18 and 16 kDa, respectively), which are localized in the cytosol (LC3-I) or in autophagosomal membranes (LC3-II). LC3-II thus can be used to estimate the abundance of autophagosomes before they are destroyed through fusion with lysosomes (29, 51). Similarly, LC3-green fluorescent protein (GFP) fusion protein redistributes from a diffuse to a vacuolar pattern when AV are formed (29, 51). Finally, Beclin 1 is the mammalian orthologue of yeast Atg6 (45). Beclin 1 localizes to the trans-Golgi network, belongs to the class III phosphatidylinositol 3-kinase complex, and participates in autophagosome formation (33, 45). Beclin 1 is monoalleli-

* Corresponding author. Mailing address: CNRS-UMR 8125, Institut Gustave Roussy, Pavillon de Recherche 1, 39 rue Camille-Desmoulins, F-94805 Villejuif, France. Phone: 33-1-42 11 60 46. Fax: 33-1-42 11 60 47. E-mail: kroemer@igr.fr.

‡ P.B. and R.-A.G.-P. contributed equally to this work.

† Supplemental material for this article may be found at http://mcb.asm.org/.

§ Present address: Consejo Superior de Investigaciones Científicas, E-28040 Madrid, Spain.

cally deleted in many human patients with sporadic breast, ovarian, and prostate cancer (45). Moreover, Beclin $1^{+/-}$ mutant mice show a high incidence of spontaneous tumors and decreased autophagy in vitro (60, 76), suggesting that autophagy (and perhaps autophagic cell death) may prevent cellular transformation (13).

We previously observed that lysosomotropic agents can lead to cytoplasmic vacuolization and cell death that involves hallmarks of apoptosis (6, 7). We therefore explored the relationship between autophagic vacuolization and subsequent cellular demise. Unexpectedly, we found that the accumulation of AV that is typical for the morphology of type 2 cell death can be due to an actual inhibition of macroautophagy at the level of the fusion between autophagosomes and lysosomes and that this accumulation by itself is not lethal. Rather, in numerous instances, induction of autophagic vacuolization ultimately triggers a cell death program that is suppressed by MMP inhibitors or caspase antagonists. Thus, biochemical hallmarks of type 1 cell death may be involved in the execution of morphological type 2 cell death, pointing to a major cross talk between the two lethal subroutines.

MATERIALS AND METHODS

Cell lines and culture conditions. HeLa cells were stably transfected with the pcDNA3.1 control vector (Neo), human Bcl-2 (Bcl-2), or the cytomegalovirus UL37 exon 1 gene coding for the viral mitochondrial inhibitor of apoptosis (vMIA, kindly provided by V. Goldmacher) (3, 19). Cells were cultured in Dulbecco modified Eagle medium supplemented with 10% fetal calf serum (FCS), 1 mM pyruvate, and 10 mM HEPES at 37°C under 5% CO_2. Simian virus 40-transformed mouse embryonic fibroblasts whose genotype was either wild type or double knockout (DKO), provided by S. Korsmeyer (69), were cultivated in Dulbecco modified Eagle medium (Life Technologies) supplemented with 10% FCS–1× nonessential amino acids (Sigma) at 37°C under 5% CO_2.

Transfection and RNA interference. Small interfering RNAs (siRNAs) were synthesized by Proligo France SAS. For *Beclin 1* (National Center for Biotechnology Information accession number AF077301), RNA sequences started at positions 189 (CUCAGGAGAGGAGCCAUUU) and 1206 (GAUUGAAGAC ACAGGAGGC) from ATG (oligoribonucleotides Beclin 100 [B110] and Beclin 168 [B168], respectively); for *Atg5* (accession number BC002699), the sequence started at position 453 (GCAACUCUGGAUGGGAUUG); for *Atg10* (accession number NM_031482), the sequence started at position 391 (GGAGUUCAUG AGUGCUAUA); and for *Atg12* (accession number NM_004707), the sequence started at position 131 (CAGAGGAACCUGCUGGCGA). As controls, siRNA ribonucleotides scrambled from B110 and targeting the unrelated protein emerin (25) were used. Cells were cultured in six-well plates and transfected at 80% confluence with Oligofectamine reagent (Invitrogen) according to the manufacturer's instructions. After 3 h, 10% FCS was added, and cells were left for another 24 to 48 h before they were trypsinized and used for experiments. Transient transfection was performed with Lipofectamine 2000 reagent (Invitrogen), and cells were used 24 h after transfection. The formation of AV was followed by means of an LC3-GFP plasmid (29). To label lysosomes, we used the SytVII-GFP plasmid (kindly provided by N. W. Andrews) (49) and lgp120-GFP (provided by J. Lippincott-Schwartz) (57). Mitochondria were labeled with the commercial mitochondrion-targeted DsRed (mtDsRed) plasmid (Clontech).

RNA extraction and quantitative RT-PCR. mRNA preparations were obtained with the RNeasy mini kit (QIAGEN) and quality controlled with an Agilent 2100 bioanalyzer (Agilent Technologies). For quantitative reverse transcription (RT)-PCR, cDNAs were synthesized from 1 μg of total RNA with Moloney murine leukemia virus reverse transcriptase (Roche). Then, the TaqMan Universal PCR was performed on an ABI PRISM 7000 sequence detection system (Applied Biosystems), according to the manufacturer's instructions, using primers specific for *Atg5*, *Atg10*, and *Atg12* (TaqMan assays reagents from Applied Biosystems).

Reagents and cell death induction. Hydroxychloroquine (HCQ; Sanofi-Synthelabo) was used from a stock solution at 30 μg/ml unless otherwise specified. Bafilomycin A1 (Baf A1; 0.1 μM; Sigma), monensin (10 μM; Calbiochem), 3-methyladenine (3-MA; 10 mM; Fluka), staurosporine (STS; 100 nM; Sigma). Anti-CD95 (200 nM; Immunotech) was used in combination with cycloheximide (1 μg/ml). For caspase inhibition, *N*-benzyloxycarbonyl-Val-Ala-Asp-fluoromethylketone (Z-VAD-fmk; Bachem) was added at the same time as cell death inducers at 25 μM (8).

Flow cytometry and cell sorting. The following fluorochromes were employed to determine apoptosis-associated changes by cytofluorometry: 3,3′-dihexyloxacarbocyanine iodide [$DiOC_6(3)$, 40 nM] for mitochondrial transmembrane potential ($\Delta\Psi_m$) quantification, propidium iodide (PI; 1 μg/ml) and 44,6-diamino-2-phenylindole (DAPI; 2.5 μM) for determination of cell viability (all from Molecular Probes), and annexin V conjugated with fluorescein isothiocyanate (Bender Medsystems) for the assessment of phosphatidylserine (PS) exposure (10, 77). To label lysosomes, LysoTracker Red (LTR; 500 nM; Molecular Probes) was used. Cells were trypsinized and labeled with the fluorochromes at 37°C, followed by cytofluorometric analysis with a fluorescence-activated cell sorter (FACS) scan (Becton Dickinson). For cell sorting, HeLa cells were treated with 60 μg of HCQ/ml for 8 h, trypsinized, and labeled with LTR, $DiOC_6(3)$, and DAPI for 15 min at 37°C, followed by purification with a Vantage FACS (Becton Dickinson). After being sorted, the different populations were either fixed (for assessment of cytochrome *c* relocation), relabeled, and reanalyzed for $DiOC_6(3)$, LTR, and DAPI or cultured again in complete medium (CM) at 37°C for 16 h.

Light microscopy and immunofluorescence. Cells cultured on coverslips were stained with Cell Tracker Green 5-chloromethylfluorescein diacetate (CMFDA; 1 μM; Molecular Probes) and Hoechst 33342 (2 μM; Sigma), followed by fluorescence microscopic assessment with a Leica IRE2 microscope equipped with a Leica DC300F camera. For Giemsa staining, cells were fixed in methanol and stained with a kit from Sigma. Alternatively, cells were fixed with paraformaldehyde (4%, wt/vol) and picric acid (0.19%, vol/vol) for LC3-GFP and immunofluorescence assays (15). Cells were stained for the detection of cytochrome *c* (monoclonal antibody 6H2.B4 from Pharmingen), LAMP2 (monoclonal antibody H4B4 from Affinity BioReagents), or activated caspase-3 (polyclonal antibody from Cell Signaling Technology), developed by goat anti-mouse or anti-rabbit immunoglobulin Alexa fluor conjugates (Molecular Probes) (12). Confocal microscopy was performed with a Zeiss LSM 510 microscope equipped with a 63× objective. To determine the percentage of colocalization, green and merged images were loaded into Image J software and the ratio of green to merged cells was determined with the colocalization plug-in. Scale bars indicate 10 μm.

Electron microscopy. Cells were fixed for 1 h at 4°C in 1.6% glutaraldehyde in 0.1 M Sörensen phosphate buffer (pH 7.3), washed and fixed again in aqueous 2% osmium tetroxide, and embedded in Epon. Electron microscopy was per-

FIG. 1. HCQ-mediated induction of acidic vacuoles. (A and B) Vacuolar acidic compartment- and apoptosis-associated parameters in HCQ-treated cells. HeLa cells were exposed to HCQ (30 μg/ml) for the indicated periods, and cells were stained with LTR, $DiOC_6(3)$, annexin V-fluorescein isothiocyanate, or PI, followed by FACS analysis. Data shown are representative FACS profiles (A) or means of results from five independent experiments ($x \pm$ standard errors of the mean [SEM]) (B). Bars in panel A indicate the window representing each population. CRT, control. (C) Effect of mitochondrion-stabilizing proteins on LTR staining. HeLa cells stably transfected with Bcl-2 or vMIA were incubated for 5 h with HCQ, followed by LTR staining and FACS analysis. Vector-only control cells (unpublished results) behaved as cells for which results are shown in the leftmost graph of panel A. (D and E) Light microscopic evidence for HCQ-induced vacuolization. Cells treated with HCQ for the indicated periods were stained with Giemsa (D) or Cell Tracker Green CMFDA (E). The arrow indicates the apoptotic nucleus. (F) Staining of lysosomes with a LAMP2 antibody. HCQ-treated HeLa cells were immunofluorescence stained and counterstained with Hoechst 33324. (G) Chronological hierarchy of vacuolization and MMP. Cells were stained with CMFDA, an anti-cytochrome *c* (Cyt *c*) antibody (revealed as red fluorescence), and Hoechst 33342 (blue fluorescence), and the frequencies of cells with enhanced vacuolization, mitochondrion-released cytochrome *c*, and apoptotic nuclei were determined ($x \pm$ SEM; $n = 4$).

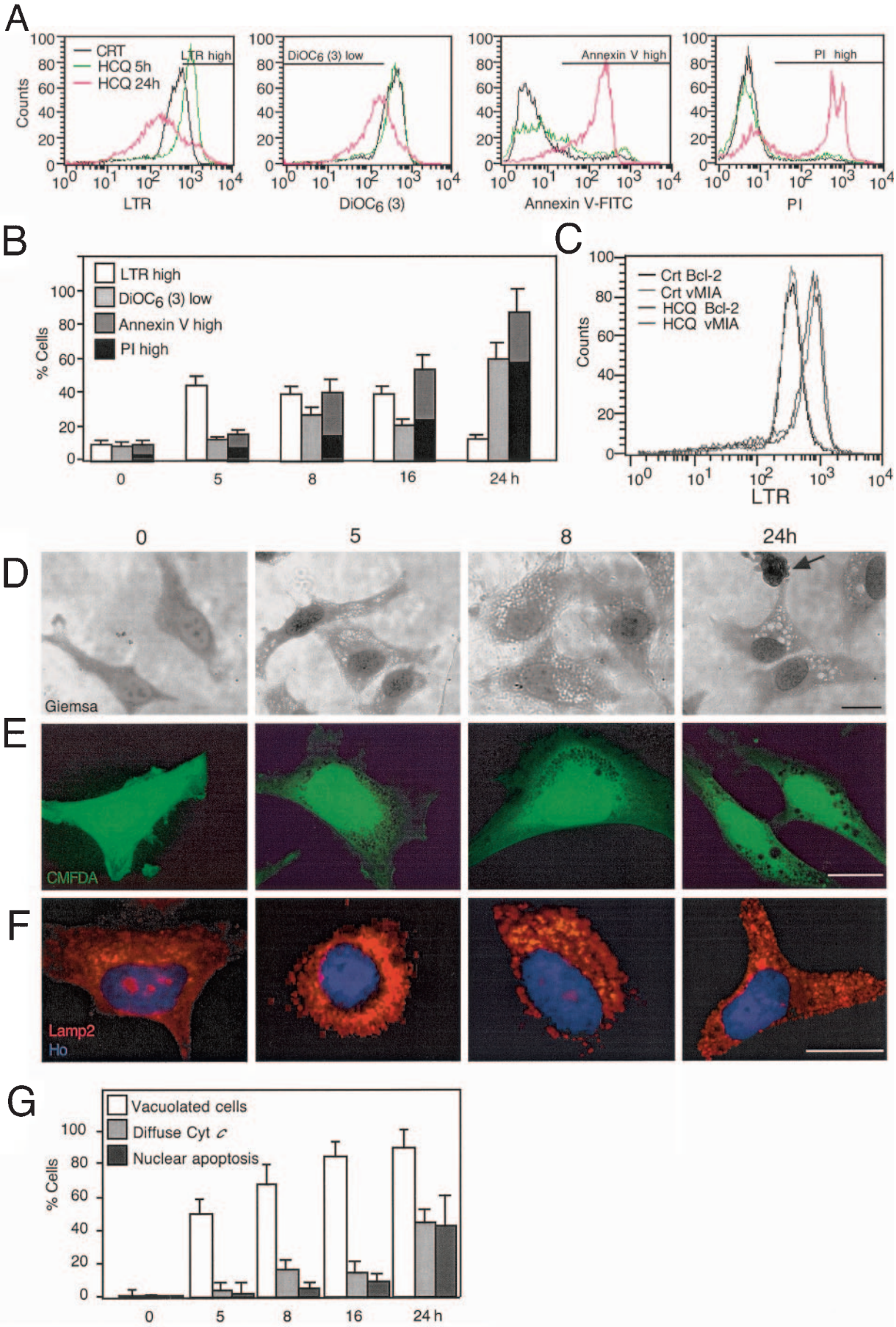
A
CRT
HCQ 5h
HCQ 24h
LTR high
Counts
LTR
DiOC6 (3) low
DiOC6 (3)
Annexin V high
Annexin V-FITC
PI high
PI
B
LTR high
DiOC6 (3) low
Annexin V high
PI high
% Cells
0
5
8
16
24 h
C
Crt Bcl-2
Crt vMIA
HCQ Bcl-2
HCQ vMIA
Counts
LTR
0
5
8
24h
D
Giemsa
E
CMFDA
F
Lamp2
Ho
G
Vacuolated cells
Diffuse Cyt c
Nuclear apoptosis
% Cells
0
5
8
16
24 h

formed with a Zeiss EM 902 transmission electron microscope, at 90 kV, on ultrathin sections (80 nm thick) stained with uranyl acetate and lead citrate. Quantification of AV was performed as described previously (65).

Western blot analysis. Cells were washed in cold phosphate-buffered saline (PBS) at 4°C and lysed in a buffer containing 50 mM Tris HCl (pH 6.8), 10% glycerol, 2% sodium dodecyl sulfate, 10 mM dithiothreitol, and 0.005% blue bromophenol. Forty micrograms of protein was loaded on a 15% sodium dodecyl sulfate–polyacrylamide gel and transferred to nitrocellulose. The membrane was incubated for 1 h in PBS-Tween 20 (0.05%) containing 5% nonfat milk. Primary antibodies (LC3 and Beclin 1; Santa Cruz Biotechnology) and activated caspase-3 (Cell Signaling Technology) were revealed with the appropriate horseradish peroxidase-labeled secondary antibodies (Southern Biotechnologies Associates) and detected by SuperSignal West Pico chemiluminescent substrate (Pierce). Anti-GAPDH (glyceraldehyde-3-phosphate dehydrogenase; Chemicon) was used to ensure equal loadings.

Analysis of protein degradation. HeLa cells were incubated with 0.2 μCi of L-valine (Perkin-Elmer Life Science)/ml in CM for 24 h (54). Unincorporated radioisotope was removed by three rinses with PBS (pH 7.4). Cells were then incubated in nutrient-free medium (NF) plus 0.1% bovine serum albumin in the presence of 10 mM cold valine for 18 h (prechase period). After this time, the media were replaced by the appropriate fresh medium plus cold valine (10 mM) in the presence of 10 mM 3-MA and 60 μg of HCQ/ml for 4 h (chase period). Cells and radiolabeled proteins were precipitated in 10% (vol/vol) trichloroacetic acid at 4°C. The precipitated proteins were separated from the soluble radioactivity by centrifugation at 600 × *g* for 20 min and then dissolved in Soluene 350. The rate of protein degradation was calculated as the level of acid-soluble radioactivity recovered from both cells and media (58).

Statistical analysis. Data were analyzed with JMP IN 4 software using one-way analyses of variance. Differences between the control and treated samples were analyzed by using individual contrasts when the factor consisted of more than two levels. *P* values of <0.05 were considered statistically significant.

RESULTS AND DISCUSSION

Prelethal accumulation of AV in HCQ-treated cells. HeLa cells exposed to the lysosomotropic agent HCQ manifested a transiently increased level of staining with LTR (LTR^{high} cells) (Fig. 1A); LTR is a fluorochrome which measures the volume of the acidic vacuolar compartment (14, 18). This increased LTR labeling was observed well before the $\Delta\Psi_m$ [as measured with $DiOC_6(3)$, a $\Delta\Psi_m$-sensitive dye] dropped, before PS residues were exposed on the plasma membrane surface (quantified with an annexin V-fluorescein isothiocyanate conjugate), and before irreversible plasma membrane permeabilization (determined with PI) occurred (Fig. 1B). Overexpression of two unrelated MMP-inhibitory proteins (Bcl-2 and vMIA) (19) retarded the acquisition of apoptotic parameters ($\Delta\Psi_m$ loss, PS exposure, and membrane permeabilization) induced by HCQ (reference 7 and unpublished results). However, Bcl-2 and vMIA did not affect LTR staining (Fig. 1C), indicating that the increase in the acidic vacuolar compartment is an upstream preapoptotic event. In addition, HCQ-treated cells manifested cytoplasmic vacuolization, as determined by Giemsa staining (Fig. 1D). Such cytoplasmic vacuoles were also detectable as "holes" not staining with CMFDA (Fig. 1E) and correlated with an increase in the volume of vesicles exhibiting a positive immunofluorescence for the lysosomal marker LAMP2 (Fig. 1F). Vacuolization occurred well before cytochrome *c* was released from mitochondria (Fig. 1G) and before nuclei condensed (Fig. 1D to F). Double staining with LTR and $DiOC_6(3)$ revealed that the increase in LTR staining, observed 8 h after HCQ addition, affected only the $DiOC_6(3)^{high}$ population of cells (Fig. 2A), correlating with an increased dispersion of light (side scatter), which suggests an elevated degree of vacuolization (Fig. 2B). FACS-sorted LTR^{high} [and hence $DiOC_6(3)^{high}$] cells contained double-membraned (that is, bona fide autophagic) vacuoles filled with cytoplasmic material yet lacked any ultrastructural sign of chromatin condensation (Fig. 2C). This phenotype was observed in the vast majority (>95%) of cells of the LTR^{high} population. In contrast, $DiOC_6(3)^{low}$, still-viable (DAPI-excluding) cells showed empty (presumably apoptotic) vacuoles in addition to the autophagic ones and underwent pyknosis and karyorrhexis (Fig. 2C and D). Accordingly, kinetic experiments revealed that HCQ-induced vacuolization, as determined by electron microscopy, led first to the accumulation of AV and then to that of empty vacuoles (Fig. 2E). Importantly, the FACS-purified LTR^{high} population did not progress to a loss in $\Delta\Psi_m$ when it was recultured overnight in CM and maintained the integrity of its plasma membrane (as determined with the vital dye DAPI), whereas $DiOC_6(3)^{low}$ cells progressively died upon reculture (Fig. 2F). Accordingly, LTR^{high} [but not $DiOC_6(3)^{low}$] cells retained cytochrome *c* in their mitochondria, even after reculture (Fig. 2G). All together, these data suggest that AV accumulation (and a transient phase of LTR^{high} staining) precedes the $\Delta\Psi_m$ loss (accompanied by a loss of LTR^{high} staining), which marks the point of no return and imminent cell death as well as apoptotic vacuolization.

In conclusion, it appears that HCQ-induced AV accumulation by itself is not sufficient to induce cell death. However, after a latency period, HCQ does induce a type of cell death that bears some hallmarks of apoptosis, such as $\Delta\Psi_m$ dissipation, cytochrome *c* translocation, and chromatin condensation.

FIG. 2. Determination of the point of no return of HCQ-induced cell death. (A) Cytofluorometric purification of subpopulations. Cells left untreated (control) or treated with HCQ (8 h, 60 μg/ml) were simultaneously stained with LTR, $DiOC_6(3)$, and the vital dye DAPI. The cells (gated on $DAPI^{low}$ events with normal forward scatter) were then subjected to FACS. The gates shown in panels A indicate the FACS-sorted populations [control, cells incorporating normal levels of LTR (LTR^{N}), LTR^{high}, and $DiOC_6(3)^{low}$ cells]. Note that the definition of LTR^{high} cells is more restrictive than in Fig. 1A. (B) Side scatter characteristics (SSC) of cells sorted in panels A. CRT, control. (C) Representative electron microscopic images obtained from such sorted cells as shown in panels A and B. Bars indicate 1 μm. E, empty vesicle; N, nucleus. Arrows indicate double membranes. (D) Quantitation of vacuolization patterns as determined by electron microscopy (50 replicates). Either the number of vesicles (autophagic vesicles, AV, or empty vesicles) per cell was determined or the percentage of the cell volume occupied by vesicles was measured by morphometry. CO, control. (E) Quantitation of vacuolization patterns of cells exposed to HCQ (60 μg/ml) without FACS purification. (F and G) Mortality of FACS-purified populations. Cells purified as described for panels A were either restained with $DiOC_6(3)$ and DAPI immediately after FACS purification or cultured for another 16 h, followed by $DiOC_6(3)$ and DAPI staining (F). Note that only the $DiOC_6(3)^{low}$ population tends to lose its viability and to become $DAPI^{high}$. Alternatively, cells were centrifuged on slides and subjected to immunofluorescent staining (0 h) or recultured for 16 h and then labeled with a cytochrome *c*-specific antibody (G). The frequency of cells with a diffuse staining pattern indicative of mitochondrial cytochrome *c* release is indicated in panels D ($x \pm$ SEM; $n = 3$).

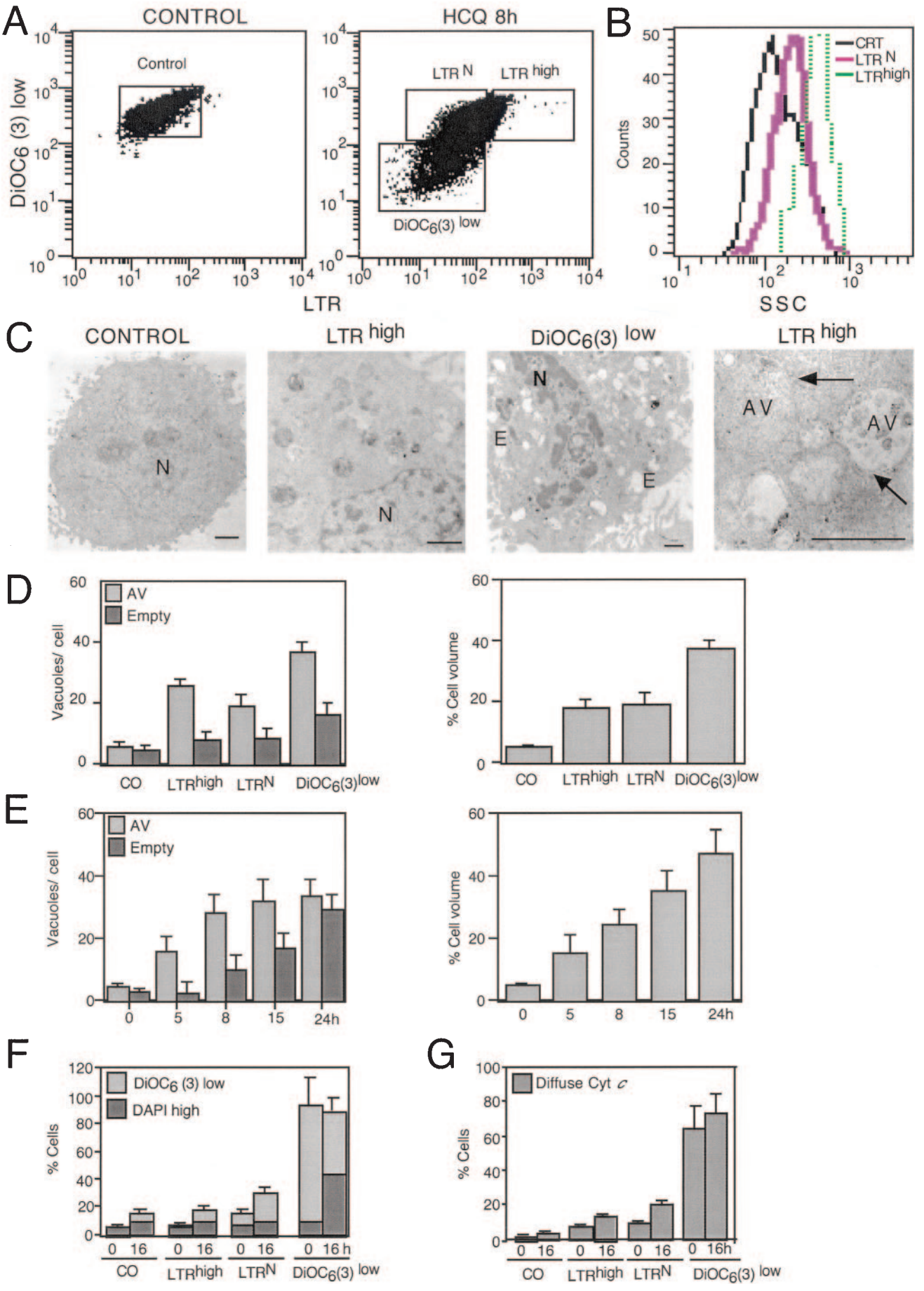
A
CONTROL
HCQ 8h
Control
LTR N
LTR high
DiOC6(3) low
DiOC6 (3) low
LTR
B
CRT
LTR N
LTRhigh
Counts
SSC
C
CONTROL
LTR high
DiOC6(3) low
LTR high
N
E
AV
D
AV
Empty
Vacuoles/ cell
% Cell volume
CO
LTRhigh
LTRN
DiOC6(3)low
E
AV
Empty
Vacuoles/ cell
% Cell volume
0
5
8
15
24h
F
DiOC6 (3) low
DAPI high
% Cells
0 16
CO
LTRhigh
LTRN
DiOC6(3) low
G
Diffuse Cyt c
% Cells
0 16
CO
LTRhigh
LTRN
DiOC6(3) low

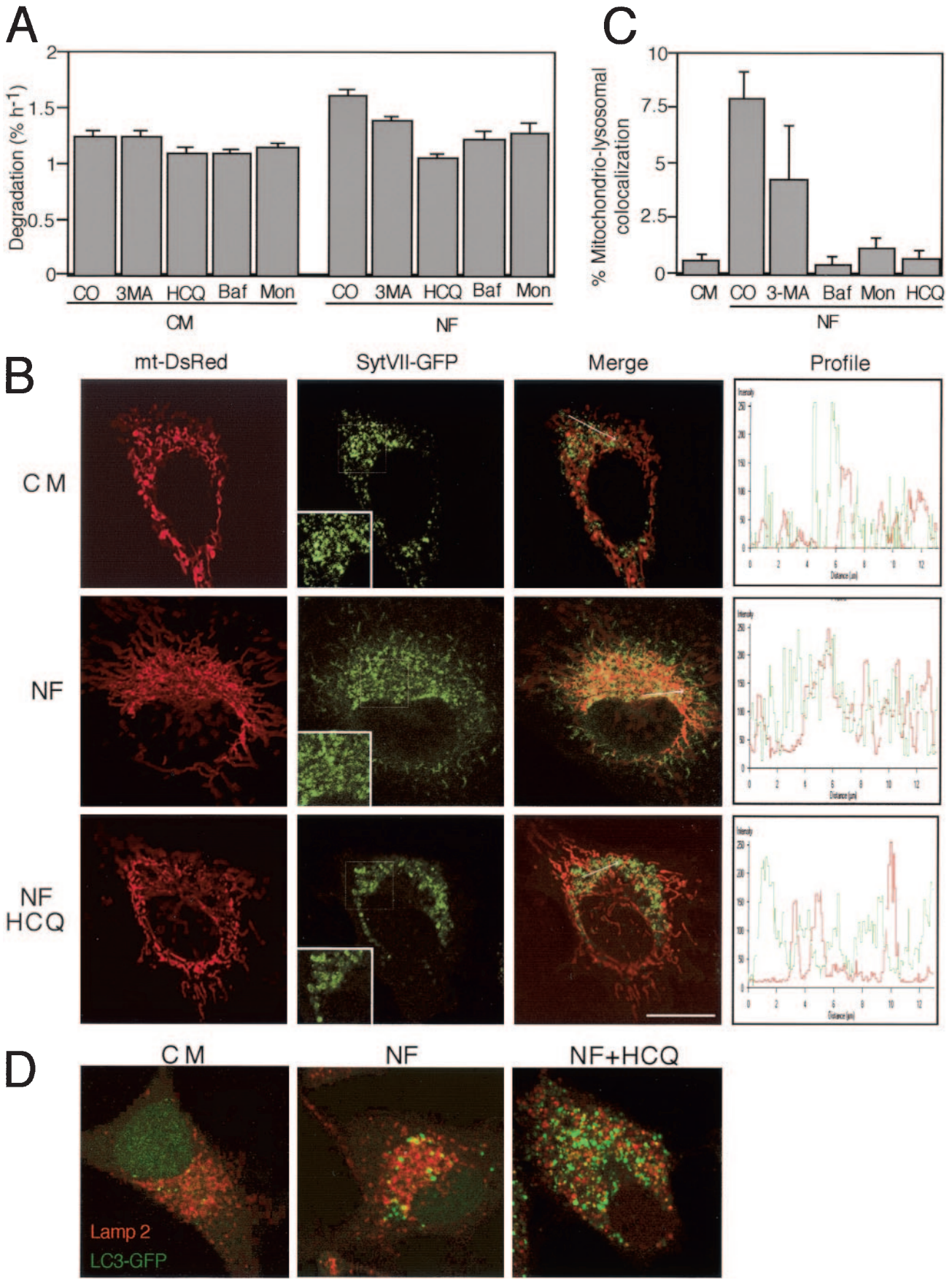
A
Degradation (% h-1)
2
1.5
1
0.5
0
CO 3MA HCQ Baf Mon
CO 3MA HCQ Baf Mon
CM
NF
C
% Mitochondrio-lysosomal colocalization
10
7.5
5
2.5
0
CM CO 3-MA Baf Mon HCQ
NF
B
mt-DsRed
SytVII-GFP
Merge
Profile
CM
NF
NF HCQ
D
CM
NF
NF+HCQ
Lamp 2
LC3-GFP

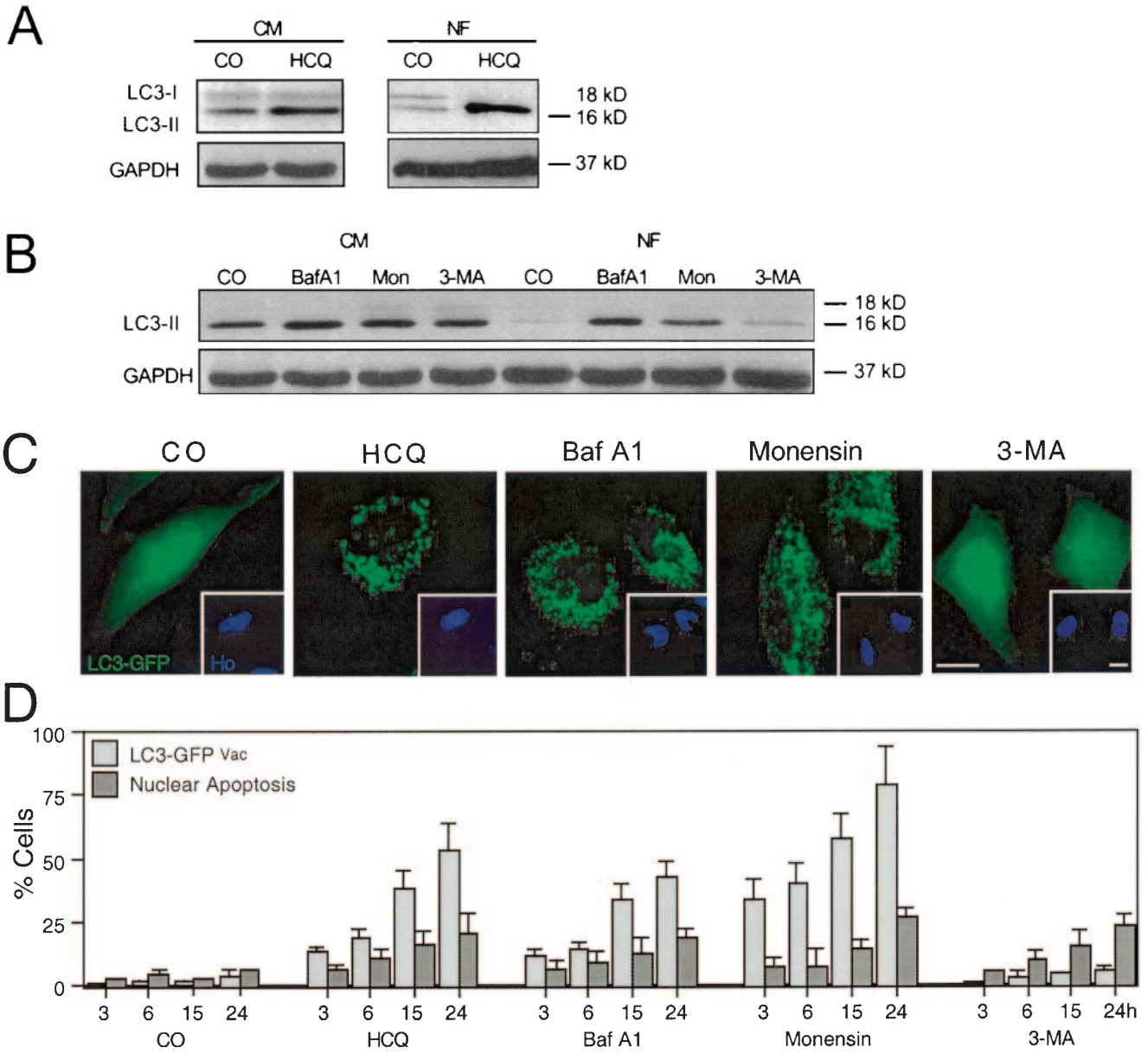

FIG. 4. Effect of HCQ and other autophagy inhibitors on the subcellular localization and biochemical status of the autophagic vacuole marker LC3. (A and B) Immunoblot analyses of accumulating LC3-II protein in control (CM) and starved (NF, 6 h) cells treated with HCQ (A) or a range of established autophagy inhibitors (B). (C and D) Redistribution of LC3-GFP. Twenty-four hours after transient transfection with an LC3-GFP chimera, cells were treated for the indicated times (24 h in panels C in the presence of serum) with HCQ, Baf A1, monensin, or 3-MA; fixed; and counterstained with Hoechst 33342. Representative cells are shown in panels C, and the frequency ($x \pm$ SEM; $n = 4$) of cells with a clear vacuolar distribution of LC3-GFP (LC3-GFP^{Vac}) or apoptotic nuclei was scored. CO, control; Mon, monensin.

FIG. 3. HCQ inhibits autophagy. (A) Effect of HCQ on protein degradation. The rate of (54) valine-labeled long-lived proteins was measured in cells incubated in either CM or NF, alone or in the presence of the indicated autophagy inhibitors. CO, control; Baf, Baf A1; Mon, monensin. (B) Effect of HCQ on the colocalization of mitochondria and lysosomes. Cells were transfected with mtDsRed and lysosome-targeted GFP (SytVII-GFP). Twenty-four hours later, cells were treated with NF (2 h) in the presence or absence of HCQ, and the cells were subjected to confocal laser microscopy. Inserts illustrate the increased size of SytVII-GFP-marked structures in HCQ-treated, nutrient-depleted cells. The graphs (right panels) represent the fluorescence distribution determined for sections of the cell, as indicated by the orientation of the arrow. (C) Quantitation of mitochondrial-lysosomal colocalization. Percentage overlaps were calculated with an image analyzer and plotted for control cells (in CM) or cells starved (in NF) in the presence of the indicated autophagy inhibitors. For results with control versus 3-MA-treated cells, P was <0.05; for results with control versus Baf A1-, monensin-, and HCQ-treated cells, P was <0.001. (D) Inhibitory effect of HCQ on the colocalization of LAMP2 and LC3-GFP. Cells transfected with LC3-GFP (24 h before the initiation of the experiment) were subjected to nutrient starvation (NF, 2 h) in the absence or presence of HCQ (30 μg/ml) and immunostained for LAMP2 detection to visualize the overlap with LC3-GFP (yellow). Representative images are shown.

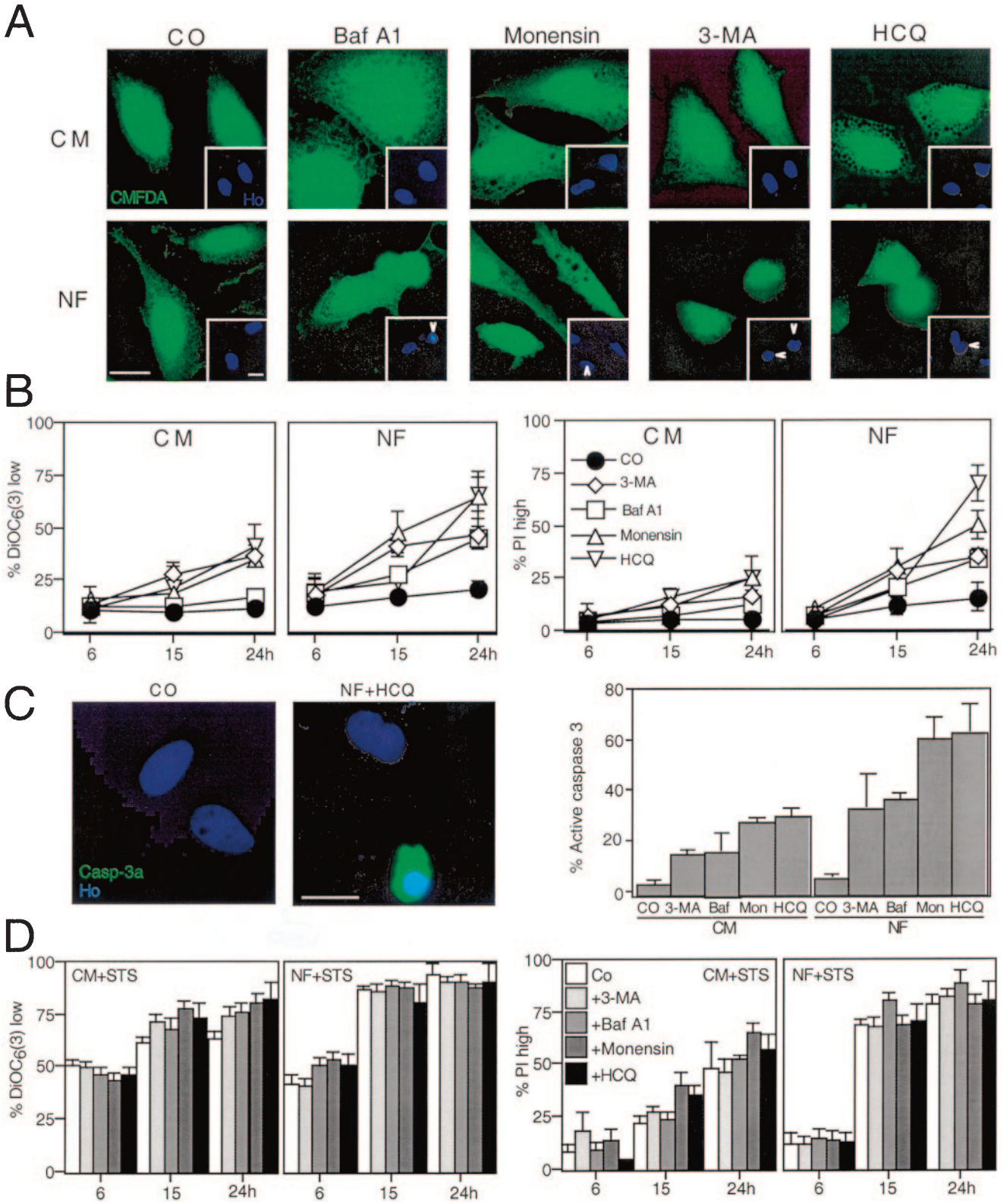

FIG. 5. Autophagy inhibition sensitizes cells to nutrient depletion-induced cell death. (A) Vacuolization induced by starvation plus autophagy inhibition. HeLa cells were cultured in CM or NF for 24 h in the presence or absence (control [CO]) of HCQ, Baf A1, monensin, or 3-MA and finally stained with CMFDA and Hoechst 33342 (inset). Note that HCQ, Baf A1, and monensin enhance the formation of AV (visible as holes in the green fluorescent staining) and induce nuclear apoptosis. Arrows mark apoptotic nuclei. (B) Quantitative assessment of synergic cell death induction. Cells cultured in CM or NF, in the presence of the indicated inhibitors or none of them (control), were stained to determine the loss of $\Delta\Psi_m$ [with $DiOC_6(3)$] and viability (with PI). Data shown are means of results of five independent experiments ± SEM. (C) Caspase-3 activation (Casp-3a) triggered by nutrient depletion plus autophagy inhibition. Cells were stained with an antibody recognizing the 17-kDa subunit of active

Pharmacological inhibition of macroautophagy precipitates starvation-induced cell death. Although HCQ induced an increase in AV (Fig. 1 and 2), it inhibited the progression of the autophagic process, based on several criteria. On the one hand, HCQ reduced the turnover of long-lived proteins, in particular in the absence of serum (Fig. 3A). On the other hand, HCQ prevented the colocalization of mitochondria and lysosomes, induced by starvation (that is, culture in serum and amino acid-free NF). Thus, nutrient-depleted cells exhibited an increased colocalization of mtDsRed- and lysosome-targeted SytVII-GFP, and this colocalization was inhibited by HCQ (Fig. 3B). Thus, HCQ acted in a fashion similar to that of other known inhibitors of autophagy, namely, Baf A1 (an inhibitor of vacuolar H^+ ATPase) (5, 74), monensin (which mediates the exchange of protons for potassium or sodium) (2, 23), and 3-MA (4, 9, 63), all of which prevented the starvation-induced colocalization of mitochondrial and lysosomal markers (Fig. 3C) and reduced the turnover of long-lived proteins (Fig. 3A). Moreover, HCQ prevented the nutrient starvation-induced colocalization of the lysosomal marker LAMP2 and the AV marker LC3-GFP (Fig. 3D) and hence prevented the formation of autophagolysosomes, as has been shown previously for Baf A1 (71).

HCQ also caused the accumulation of the AV marker LC3-II (29, 51) both in CM and under conditions of starvation, as determined by immunoblotting (Fig. 4A). This effect was again similar to that induced by Baf A1 and monensin (Fig. 4B). HCQ, Baf A1, and monensin also led to the redistribution of an LC3-GFP fusion construct into punctate cytoplasmic structures (Fig. 4C), indicating an increase in AV. Kinetic experiments revealed that the LC3-GFP redistribution to vacuoles occurred in cells well before nuclear apoptosis increased above background levels (Fig. 4D). However, all autophagy inhibitors, including 3-MA, did induce nuclear apoptosis when they were added to starved cells (Fig. 5A). While starvation alone did not cause major cell death (as defined by a loss in $\Delta\Psi_m$ or staining with PI), the combination of starvation and autophagy inhibition (with HCQ, Baf A1, monensin, or 3-MA) had a synergistic lethal effect (Fig. 5B). Similar results were obtained when PS exposure was measured (unpublished results). Moreover, we found that caspase-3 was synergistically activated by nutrient depletion and autophagy inhibition (Fig. 5C). In strict contrast, autophagy inhibition did not increase the lethal actions of classical apoptosis inducers such as STS (Fig. 5D) and the CD95 agonistic antibody 7C11 (unpublished results). As a result, it appears that pharmacological autophagy inhibition can sensitize cells to starvation-induced cell death.

Autophagic vacuolization-associated cell death is reduced by mitochondrial stabilization and caspase inhibition. To determine by which mechanism starvation coupled to autophagy inhibition killed cells, we introduced Bcl-2 and vMIA, two MMP inhibitors, into HeLa cells or used the pan-caspase inhibitor Z-VAD-fmk as an apoptosis suppressor. Bcl-2 and vMIA reduced the losses in $\Delta\Psi_m$ and viability induced by starvation plus autophagy inhibitors (Fig. 6A and B). Caspase inhibition with Z-VAD-fmk (25 μM) reduced the loss of viability induced by autophagy suppression yet had no significant effect on the loss in $\Delta\Psi_m$ (Fig. 6A and B), suggesting that, as in other paradigms of apoptosis (21, 22, 38), caspase activation occurred downstream of MMP. Of note, neither MMP nor the caspase inhibitors (Bcl-2, vMIA, and Z-VAD-fmk) affected the formation of AV, as determined by assessing the autophagosomal redistribution of LC3-GFP induced by HCQ (Fig. 6C), Baf A1, or monensin (see Fig. S1 in the supplemental material) in the presence or absence of serum. To further substantiate the role of MMP in the death process, we used mouse embryonic fibroblasts that lacked both the proapoptotic multidomain Bcl-2 family proteins Bax and Bak (DKO) cells. While DKO cells failed to die, wild-type control cells readily succumbed to starvation plus treatment with HCQ, Baf A1, monensin, or 3-MA (Fig. 7A and B). However, the absence of Bax and Bak did not inhibit vacuolization induced by HCQ, monensin (Fig. 7C), or Baf A1 (see Fig. S2 in the supplemental material) in the absence or presence of serum. All together, these data indicate that two biochemical processes that define apoptosis (MMP and caspase activation) are required for the demise of starved, autophagy-inhibited cells.

Knockdown of essential components of the autophagic machinery sensitizes cells to starvation-induced death. Pharmacological inhibition of autophagy might be affected by nonwarranted side effects of drugs endowed with limited selectivity. Therefore, we used siRNA to knock down *Atg* genes implicated in the autophagic pathway. First, we targeted the essential *Beclin 1*/*Atg6* gene (45). Two different siRNA constructs designed to down-regulate the expression of Beclin 1 (Fig. 8A) reduced the colocalization of mitochondria and lysosomes induced by starvation compared to the level of colocalization produced by a scrambled siRNA control (Fig. 8B). This manipulation also enhanced the losses in $\Delta\Psi_m$ and viability induced by starvation yet had no effect on cell death induction by the universal apoptosis inducer STS (Fig. 8C). Addition of the broad-spectrum caspase inhibitor Z-VAD-fmk (Fig. 8C) or transfection with Bcl-2 or vMIA (Fig. 8D) had a selective effect on viability (with inhibitory effects of Z-VAD-fmk, Bcl-2, and vMIA) and $\Delta\Psi_m$ dissipation (with inhibition by Bcl-2 and vMIA yet no effect by Z-VAD-fmk). Since Beclin 1 has been shown to interact with Bcl-2 (45), it might have been possible that the Beclin 1 effects involved direct cross talk with mitochondria. We therefore used siRNA constructs designed to target other *Atg* genes (*Atg5*, *Atg10*, and *Atg12*) (Fig. 9A), which did prevent mitochondrial-lysosomal colocalization (Fig. 9B). siRNA of these *Atg* gene products enhanced starvation-induced cell death (but not STS-mediated killing). Cooperative killing of *Atg5*, *Atg10*, or *Atg12* by starvation plus treatment with siRNA was inhibited by Z-VAD-fmk (which, however,

caspase-3, and the frequency of positive cells was scored after culture in the presence or absence of nutrient and autophagy inhibitors (as described for panel B, at 24 h). Ho, Hoechst 33342; Baf, Baf A1; Mon, monensin. (D) Autophagy inhibition does not sensitize cells to STS-induced cell death. Cells were cultured with 100 nM STS in the presence of the indicated inhibitors, and cell death-related parameters were measured as described for panels B. Results are mean values ± SEM of three to five independent determinations.

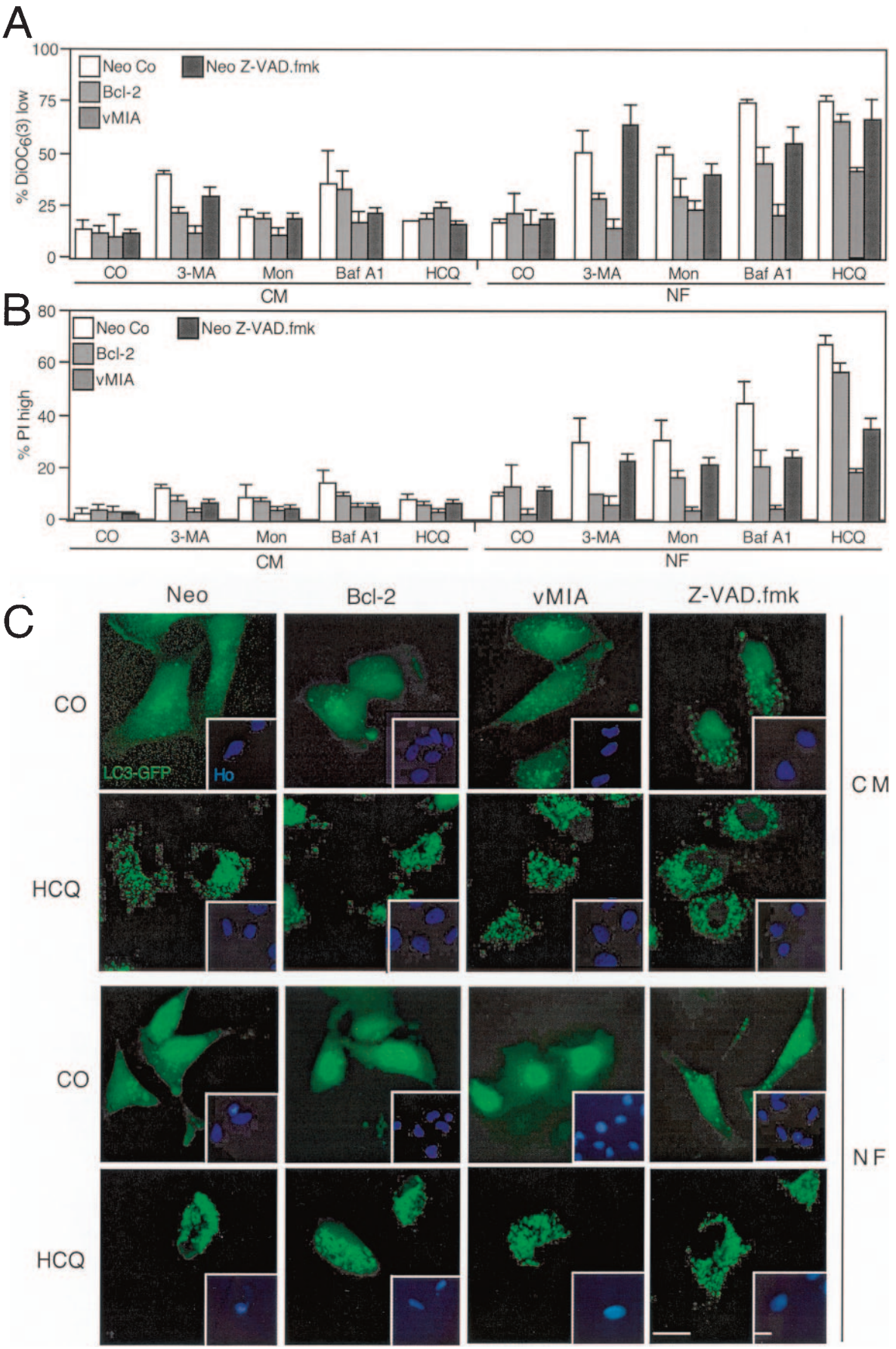
A
100
75
50
25
0
% DiOC6(3) low
Neo Co
Neo Z-VAD.fmk
Bcl-2
vMIA
CO
3-MA
Mon
Baf A1
HCQ
CM
NF
B
80
60
40
20
0
% PI high
C
Neo
Bcl-2
vMIA
Z-VAD.fmk
LC3-GFP
Ho
CM
NF

had no effect on the disruption of the $\Delta\Psi_m$) (Fig. 9C). Again, both Bcl-2 and the mitochondrion-targeted viral inhibitor vMIA prevented death acceleration by the knockdown of diverse Atg genes (Fig. 9D). Thus, siRNA experiments confirmed the cytoprotective potential of autophagy under conditions of starvation and extended the notion that impaired autophagy can kill nutrient-deprived cells by an apoptotic mechanism.

Concluding remarks. In the present paper, we demonstrate that the death-associated accumulation of AV may be the result of inhibited rather than exacerbated autophagy. Inhibition of the fusion of lysosomes with autophagosomes by HCQ, Baf A1, or monensin results in the accumulation of AV, which was detectable at several levels (LC3 proteolysis in Fig. 4A, LC3-GFP redistribution in Fig. 4C, extension of the acidic compartment in Fig. 1 and 3, accumulation of two-membraned vesicles in Fig. 2, cytoplasmic vacuolization in Fig. 1D and E, increase in the volume of LAMP2-positive vesicles in Fig. 1F, and increase in the volume of Syt VII-GFP-labeled vesicles in Fig. 3B). HCQ (Fig. 3D), Baf A1 (71), and monensin (data not shown) apparently inhibited the formation of autophagolysosomes through the fusion of AV and lysosomes, thereby reducing the turnover of AV. This reduction in turnover is linked to enhanced cell death, in particular under conditions of nutrient depletion (Fig. 5). Although autophagic vacuolization by itself is not lethal (Fig. 2), it primes cells for death accompanied by a loss in the $\Delta\Psi_m$ (which marks the point of no return) (Fig. 2), relocation of cytochrome *c* from mitochondria to the cytosol (Fig. 2G), caspase activation (Fig. 5C), PS exposure (Fig. 1A and B), and terminal plasma membrane permeabilization (Fig. 1A and B and 5B). Similarly, inhibition of the early stages of autophagy, using 3-MA (Fig. 3 to 7) or more specifically siRNA for the knockdown of Atg5, Atg6/Beclin 1, Atg10, and Atg12 (Fig. 8 to 9), sensitized cells to starvation-induced cell death, although without any signs of autophagic vacuolization. Irrespective of the stage at which autophagy was inhibited, disabled autophagy accelerated starvation-induced death via a common final pathway involving biochemical features of apoptosis. Thus, mitochondrial stabilization (by overexpressed Bcl-2 or vMIA in Fig. 6A and B, 8C and D, and 9D or by knockout of Bax and Bak in Fig. 7) or caspase inhibition (Fig. 6A to C, 8C, and 9C) succeeded in delaying cell death induced by combined starvation and autophagy suppression.

How is it possible that apoptosis is initiated by suppressed autophagy? In a variety of systems, disequilibria in defined organellar systems leads to local caspase activation (e.g., caspase-12 in the endoplasmic reticulum and caspase-2 in the nucleus) (16, 40, 52). However, caspase activation is probably not an initiating event in this system, because Z-VAD-fmk does not affect MMP (Fig. 6A, 8C, and 9D), which thus is likely to occur upstream and independently from caspases. It remains an ongoing conundrum how MMP occurs in starvation-induced cell death under conditions of autophagy inhibition. Although Bax and Bak are clearly involved in this process (Fig. 8), it is unclear which upstream processes may account for Bax- or Bak-mediated MMP. On theoretical grounds, MMP may result from bioenergetic failure (59), perhaps as a result of nutrient depletion, combined with the impossibility of recruiting endogenous nutrients by autophagy-dependent catabolic reactions. Furthermore, autophagy is the process that leads to the removal of damaged mitochondria, provided that MMP occurs at a level below the apoptotic threshold (14). Thus, it is conceivable that failure to remove individual mitochondria that undergo MMP primes for apoptosis. In addition, or alternatively, the inhibition of autophagy might alter the equilibrium state between pro- and antiapoptotic mediators with different half-lives, much as this has been shown for proteasome inhibition, a manipulation that induces apoptosis via multiple (and perhaps inextricable) pathways (11, 28, 44, 50, 64, 67).

Irrespective of the detailed molecular pathways linking disabled autophagy to mitochondrial apoptosis, the results contained in this work add to the growing suspicion that type 1 and type 2 cell death may be somehow interwoven. Thus, in *Drosophila* development, the involution of the salivary gland—a paradigm of type 2 cell death—is actually linked to the expression of numerous proapoptotic genes (20, 41) and requires activation of caspases (48). In mammals, Beclin 1/Atg6 has been shown to interact with Bcl-2 (46), and down-regulation of Bcl-2 by the antisense approach can actually trigger type 2 cell death (62). A BH3-only protein interacting with Bcl-2, HSpin1, has also been found to induce type 2 cell death (72). DAP kinase, a well-known tumor suppressor gene (35), stimulates autophagy as well as apoptosis-related membrane blebbing (27). Finally, a series of bona fide apoptosis inducers can trigger type 2 cell death in some cell types (31, 55, 56).

Two important notions emerge from our findings. First, autophagy may preserve cellular homeostasis while suppressing the latent apoptotic program, meaning that under conditions of nutrient deprivation, autophagy can actually suppress cell death, presumably by providing endogenous metabolites when exogenous nutrients are missing. While it is not a new finding that autophagy can rescue cells under conditions of starvation (34, 37, 66), it is novel that autophagy actually prevents the apoptotic default pathway to be activated. This finding may be incorporated into a more general hypothesis suggesting the existence of a double switch between the two principal lethal

FIG. 6. Effect of apoptosis inhibitors on starvation-induced cell death occurring in autophagy-inhibited cells. (A and B) Effect of the inhibitors on cell death markers. HeLa cells stably transfected with vector only (Neo), left untreated (Neo Co), or treated with the pan-caspase inhibitor Z-VAD-fmk human or cells transfected with Bcl-2 or cytomegalovirus-derived vMIA were cultured under the indicated conditions (not starved in CM and starved in NF) in the absence (control [CO]) or presence of the indicated autophagy inhibitors for 24 h. Then, the percentages of cells ($x \pm$ SEM; $n = 4$) with low-level $DiOC_6(3)$ incorporation (A) and PI-permeable plasma membranes (B) were determined by cytofluorometry. Mon, monensin. (C) Apoptosis inhibition does not affect the accumulation of autophagosomes. Cells (Neo-, Bcl-2-, or vMIA-transfected cells as described for panels B and C) were transfected with the LC3-GFP chimera and then treated with HCQ (24 h) in the presence (CM) or absence (NF) of serum, and in the presence of Z-VAD-fmk where indicated, followed by counterstaining with Hoechst 33342 (Ho) and fluorescent microscopy.

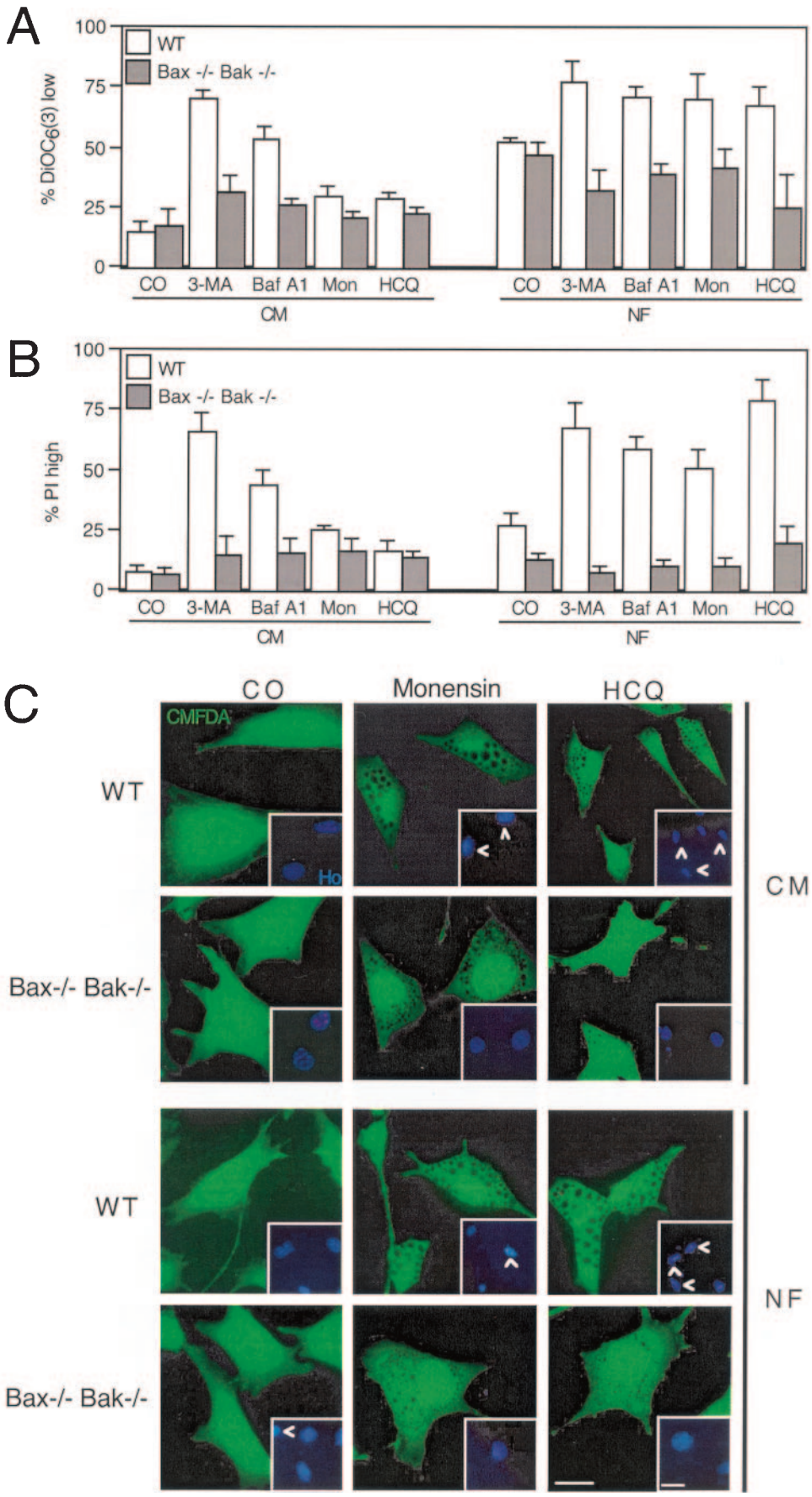
A
% DiOC6(3) low
WT
Bax -/- Bak -/-
100
75
50
25
0
CO
3-MA
Baf A1
Mon
HCQ
CM
NF
B
% PI high
C
CO
Monensin
HCQ
CMFDA
WT
Bax-/- Bak-/-
CM
NF

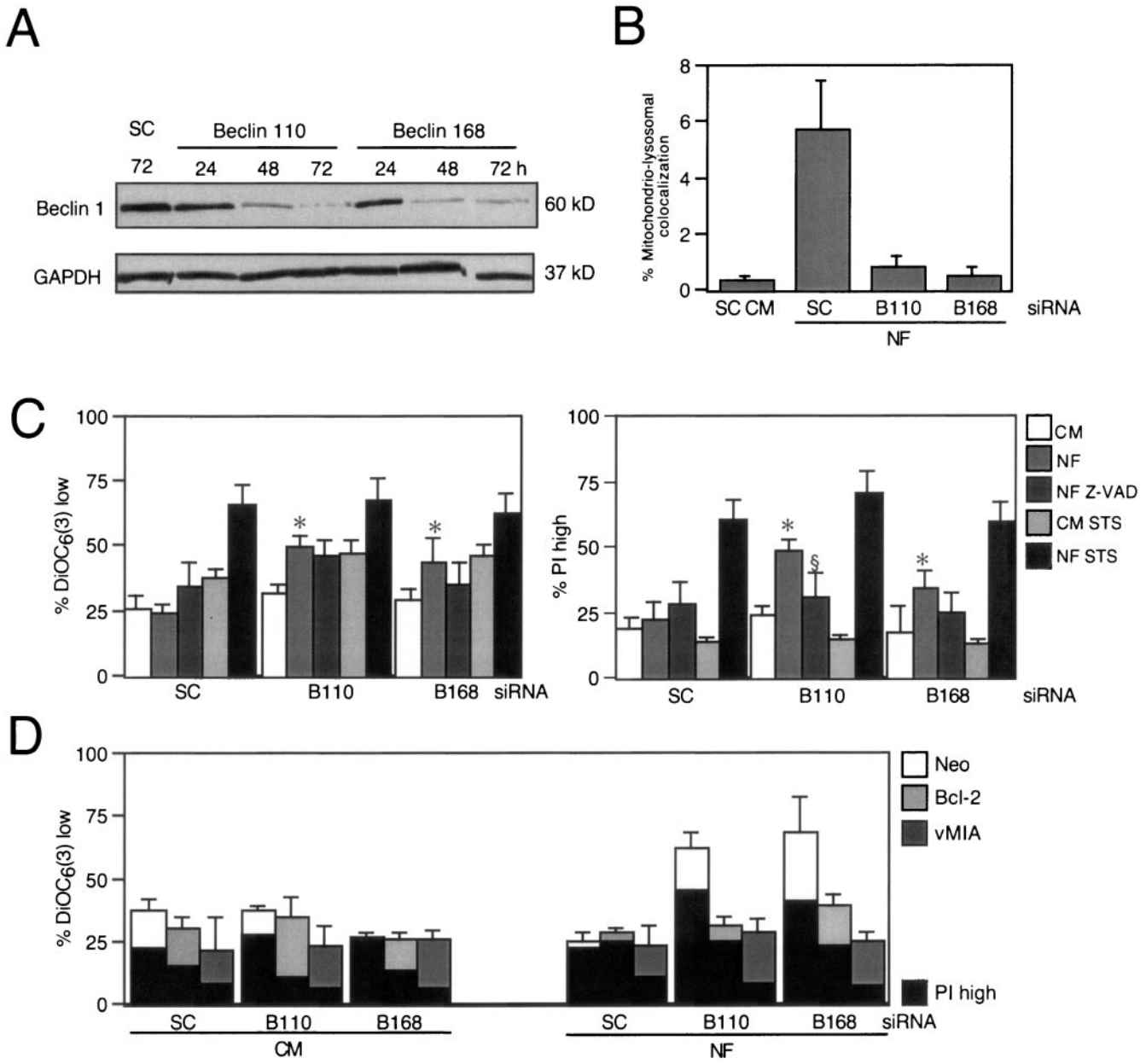

FIG. 8. siRNA of Beclin 1 sensitizes cells to starvation-induced cell death. (A) siRNA-induced downregulation of Beclin 1, determined by immunoblotting at the indicated times after treatment with scrambled control (SC) siRNA or two different Beclin 1-1-targeted double-stranded oligoribonucleotides. (B) Effect of Beclin 1-specific siRNA on the colocalization of mitochondria (DsRed labeled) or lysosomes (GFP labeled) after culture in NF. The degree of colocalization ($x \pm$ SEM; $n = 12$) was determined as described for Fig. 3. (C and D) Beclin 1 knockdown sensitizes cells to nutrient depletion-induced cell death. HeLa cells that were either wild type (C) or transfected with the neomycin resistance gene, vMIA, or Bcl-2 (D) were exposed to the indicated siRNA and then cultured for 24 h in nutrient-rich (CM) or nutrient-deficient (NF) medium, in the presence (C) or absence (C and D) of Z-VAD-fmk (Z-VAD) or STS (15 h) followed by $DiOC_6(3)$ or PI staining ($x \pm$ SEM; $n = 4$). *, P was <0.05 versus values with CM; §, $P < 0.05$ versus values with NF.

FIG. 7. DKO of Bax and Bak protects against starvation-induced cell death exacerbated by autophagy inhibition. Wild-type (WT) mouse embryonic fibroblasts or Bax and Bak DKO ($Bax^{-/-}$ $Bak^{-/-}$) fibroblasts were cultured in CM or NF and incubated with 3-MA, Baf A1, monensin (Mon), or HCQ for 24 h and then stained with a low concentration of $DiOC_6(3)$ (A) or a high concentration of PI (B), followed by cytofluorometric analysis ($x \pm$ SEM; $n = 3$). Alternatively, cells were stained with CMFDA and Hoechst 333234 and observed under fluorescence microscopy. Representative images for monensin- and HCQ-treated cells (in CM or NF) are shown. CO, control.

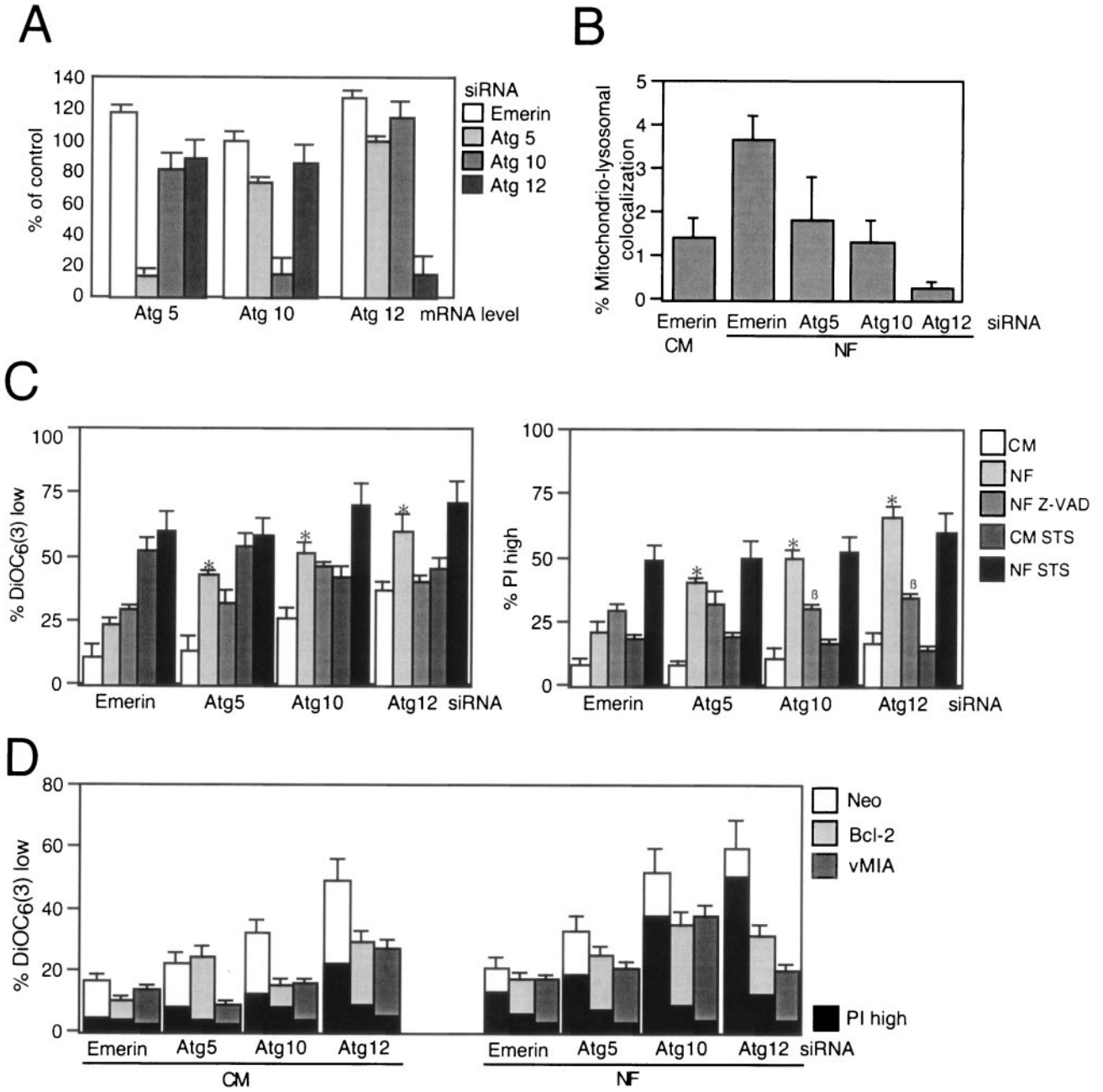

FIG. 9. Targeting of *Atg* genes enhances the lethality of nutrient depletion. (A) Reduction of mRNA levels by *Atg*-specific siRNA. After treatment with the indicated siRNA, the level of mRNA was determined by quantitative RT-PCR after 24 h. Results ($x \pm$ SEM; $n = 3$) are expressed as percentages, with 100% being considered the mRNA level of untreated control cells. (B) Effect of *Atg*-specific siRNA on the colocalization of mitochondria and lysosomes determined as described for Fig. 3B. (C and D) Apoptosis inhibition reduces cell death induced by starvation plus Atg depletion. Cells with the indicated genotype (wild type in panel C; Neo, Bcl-2, or vMIA in panel D) were treated with diverse siRNA constructs (24 h) and then starved for nutrients and/or treated with Z-VAD-fmk (Z-VAD) or STS. Data result from cytofluorometric analyses of $DiOC_6(3)$- or PI-stained cells ($x \pm$ SEM; $n = 4$). *, P was <0.05 versus values with CM; §, P was <0.05 versus values with NF.

signaling pathways. On the one hand, inhibition of apoptosis (induced by growth factor withdrawal) can lead to a chronic degenerative autophagic cell death (17, 70). On the other hand, prevention of autophagy can precipitate death, as shown here. Second, cells that exhibit morphological hallmarks of type 2 cell death with a massive AV accumulation, due to a reduced formation of autophagolysosomes, are not yet committed to cell death when mitochondria are intact. Paradoxically, such cells ultimately die from apoptosis, if we define apoptosis in biochemical terms as a process that can be inhibited by Bcl-2, vMIA, the DKO of Bax and Bak, or caspase inhibitors. Thus, the presumed mechanistic contraposition of the type 1 and type 2 forms of cell death deserves close scrutiny and critical reevaluation.

ACKNOWLEDGMENTS

We thank Jennifer Lippincott-Schwartz (Cell Biology and Metabolism Branch, National Institute of Child Health and Human Development, National Institutes of Health, Bethesda, Md.), Victor Goldmacher (ImmunoGen, Inc., Cambridge, Mass.), Stanley J. Korsmeyer (Harvard Medical School, Boston, Mass.), and Norma W. Andrews (Section of Microbial Pathogenesis and Department of Cell Biology, Yale University School of Medicine, New Haven, Conn.) for reagents; Yann Lecluse (IGR, Villejuif, France) for cell sorting; Ana-Maria Cuervo (Albert Einstein College of Medicine, Bronx, N.Y.) for helpful discussion; Patrick Fitze (Laboratory of Ecology, University Pierre and Marie Curie, Paris, France) for statistical advice; and Abdelali Jalil (Institut Gustave Roussy, Villejuif, France) for confocal microscopy.

This work has been supported by a special grant from the LNC as well as grants from the ANRS and the European Commission (QLK3-CT-2002-01956 to G.K.). P.B. received a fellowship from the European Commission (MCFI-2000-00943), as did R.-A.G.-P. (FP6-2002-5000698); N.C. and J.-L.P. received grants from the FRM and the ANRS, respectively.

REFERENCES

1. **Adams, J. M.** 2003. Ways of dying: multiple pathways to apoptosis. Genes Dev. **17:**2481–2495.
2. **Beers, M. F.** 1996. Inhibition of cellular processing of surfactant protein C by drugs affecting intracellular pH gradients. J. Biol. Chem. **271:**14361–14370.
3. **Belzacq, A. S., C. El Hamel, H. L. A. Vieira, I. Cohen, D. Haouzi, D. Métivier, P. Marchetti, V. Goldmacher, C. Brenner, and G. Kroemer.** 2001. The adenine nucleotide translocator mediates the mitochondrial membrane permeabilization induced by lonidamine, arsenite and CD437. Oncogene **20:**7579–7587.
4. **Blommaart, E. F., U. Krause, J. P. Schellens, H. Vreeling-Sindelarova, and A. J. Meijer.** 1997. The phosphatidylinositol 3-kinase inhibitors wortmannin and LY294002 inhibit autophagy in isolated rat hepatocytes. Eur. J. Biochem. **243:**240–246.
5. **Bowman, E. J., A. Siebers, and K. Altendorf.** 1988. Bafilomycins: a class of inhibitors of membrane ATPases from microorganisms, animal cells, and plant cells. Proc. Natl. Acad. Sci. USA **85:**7972–7976.
6. **Boya, P., K. Andreau, D. Poncet, N. Zamzami, J.-L. Perfettini, D. Métivier, D. M. Ojcius, M. Jaattela, and G. Kroemer.** 2003. Lysosomal membrane permeabilization induces cell death in a mitochondrion-dependent fashion. J. Exp. Med. **197:**1323–1334.
7. **Boya, P., R.-A. González-Polo, D. Poncet, K. Andreau, T. Roumier, J.-L. Perfettini, and G. Kroemer.** 2003. Mitochondrial membrane permeabilization is a critical step of lysosome-initiated apoptosis induced by hydroxychloroquine. Oncogene **22:**3927–3936.
8. **Boya, P., M. C. Morales, R.-A. González-Polo, K. Andreau, I. Gourdier, J.-L. Perfettini, N. Larochette, A. Deniaud, F. Baran-Marszak, R. Fagard, J. Feuillard, A. Asumendi, M. Raphael, B. Pau, C. Brenner, and G. Kroemer.** 2003. The chemopreventive agent 4-hydroxyphenylretinamide induces apoptosis through a mitochondrial pathway regulated by proteins from the Bcl-2 family. Oncogene **22:**6220–6230.
9. **Bursch, W.** 2001. The autophagosomal-lysosomal compartment in programmed cell death. Cell Death Differ. **8:**569–581.
10. **Castedo, M., K. Ferri, T. Roumier, D. Métivier, N. Zamzami, and G. Kroemer.** 2002. Quantitation of mitochondrial alterations associated with apoptosis. J. Immunol. Methods **265:**39–47.
11. **Chen, W. J., and J. K. Lin.** 2004. Induction of G_1 arrest and apoptosis in human Jurkat T cells by pentagalloylglucose through inhibiting proteasome activity and elevating p27Kip1, p21Cip1/WAF1, and Bax proteins. J. Biol. Chem. **279:**13496–13505.
12. **Cregan, S. P., A. Fortin, J. G. MacLaurin, S. M. Callaghan, F. Cecconi, D. S. Park, T. M. Dawson, G. Kroemer, and R. S. Slack.** 2002. Apoptosis-inducing factor is involved in the regulation of caspase-independent neuronal cell death. J. Cell Biol. **158:**507–517.
13. **Edinger, A. L., and C. B. Thompson.** 2003. Defective autophagy leads to cancer. Cancer Cell **4:**422–424.
14. **Elmore, S. P., T. Quian, S. F. Grissom, and J. J. Lemasters.** 2002. The mitochondrial permeability transition initiates autophagy in rat hepatocytes. FASEB J. **15:**2286–2287.
15. **Ferri, K. F., E. Jacotot, J. Blanco, J. A. Esté, A. Zamzami, S. A. Susin, G. Brothers, J. C. Reed, J. M. Penninger, and G. Kroemer.** 2000. Apoptosis control in syncytia induced by the HIV type 1-envelope glycoprotein complex: role of mitochondria and caspases. J. Exp. Med. **192:**1081–1092.
16. **Ferri, K. F., and G. K. Kroemer.** 2001. Organelle-specific initiation of cell death pathways. Nat. Cell Biol. **3:**E255–E263.
17. **Fletcher, G. C., L. Xue, S. K. Passingham, and A. M. Tolkovsky.** 2000. Death commitment is advanced by axotomy in sympathetic neurons. J. Cell Biol. **150:**741–754.
18. **Fuller, K. M., and E. A. Arriaga.** 2003. Analysis of individual acidic organelles by capillary electrophoresis with laser-induced fluorescence detection facilitated by the endocytosis of fluorescently labeled microspheres. Anal. Chem. **75:**2123–2130.
19. **Goldmacher, V. S., L. M. Bartle, S. Skletskaya, C. A. Dionne, N. L. Kedersha, C. A. Vater, J. W. Han, R. J. Lutz, S. Watanabe, E. D. C. McFarland, E. D. Kieff, E. S. Mocarski, and T. Chittenden.** 1999. A cytomegalovirus-encoded mitochondria-localized inhibitor of apoptosis structurally unrelated to Bcl-2. Proc. Natl. Acad. Sci. USA **96:**12536–12541.
20. **Gorski, S. M., S. Chittaranjan, E. D. Pleasance, J. D. Freeman, C. L. Anderson, R. J. Varhol, S. M. Coughlin, S. D. Zuyderduyn, S. J. Jones, and M. A. Marra.** 2003. A SAGE approach to discovery of genes involved in autophagic cell death. Curr. Biol. **13:**358–363.
21. **Green, D. R., and G. Kroemer.** 1998. The central executioner of apoptosis: mitochondria or caspases? Trends Cell Biol. **8:**267–271.
22. **Green, D. R., and J. C. Reed.** 1998. Mitochondria and apoptosis. Science **281:**1309–1312.
23. **Grinde, B.** 1983. Effect of carboxylic ionophores on lysosomal protein degradation in rat hepatocytes. Exp. Cell Res. **149:**27–35.
24. **Guimaraes, C. A., M. Benchimol, G. P. Amarante-Mendes, and R. Linden.** 2003. Alternative programs of cell death in developing retinal tissue. J. Biol. Chem. **278:**41938–41946.
25. **Harborth, J., S. M. Elbashir, K. Bechert, T. Tuschl, and K. Weber.** 2001. Identification of essential genes in cultured mammalian cells using small interfering RNAs. J. Cell Sci. **114:**4557–4565.
26. **Hernandez, L. D., M. Pypaert, R. A. Flavell, and J. E. Galán.** 2003. A *Salmonella* protein causes macrophage cell death by inducing autophagy. J. Cell Biol. **163:**1123–1131.
27. **Inbal, B., S. Bialik, I. Sabanay, G. Shani, and A. Kimchi.** 2002. DAP kinase and DRP-1 mediate membrane blebbing and the formation of autophagic vesicles during programmed cell death. J. Cell Biol. **157:**455–468.
28. **Jesenberger, V., and S. Jentsch.** 2002. Deadly encounter: ubiquitin meets apoptosis. Nat. Rev. Mol. Cell Biol. **3:**112–121.
29. **Kabeya, Y., N. Mizushima, T. Ueno, A. Yamamoto, T. Kirisako, T. Noda, E. Kominami, Y. Ohsumi, and T. Yoshimori.** 2000. LC3, a mammalian homologue of yeast Apg8p, is localized in autophagosome membranes after processing. EMBO J. **19:**5720–5728.
30. **Kanzawa, T., I. M. Germano, T. Komata, H. Iton, Y. Kondo, and S. Kondo.** 2004. Role of autophagy in temozolomide-induced cytotoxicity for malignant glioma cells. Cell Death Differ. **11:**448–457.
31. **Kanzawa, T., Y. Kondo, H. Ito, S. Kondo, and I. Germano.** 2003. Induction of autophagic cell death in malignant glioma cells by arsenic trioxide. Cancer Res. **63:**2103–2108.
32. **Kerr, J. F. R., A. H. Wyllie, and A. R. Currie.** 1972. Apoptosis: a basic biological phenomenon with wide-ranging implications in tissue kinetics. Br. J. Cancer **26:**239–257.
33. **Kihara, A., Y. Kabeya, Y. Ohsumi, and T. Yoshimori.** 2001. Beclin-phosphatidylinositol 3-kinase complex functions at the trans-Golgi network. EMBO Rep. **2:**330–335.
34. **Kim, J., and D. J. Klionsky.** 2000. Autophagy, cytoplasm-to-vacuole targeting pathway, and pexophagy in yeast and mammalian cells. Annu. Rev. Biochem. **69:**303–342.
35. **Kimchi, A.** 2001. A cell death-promoting kinase. Nat. Struct. Biol. **8:**824–826.
36. **Klionsky, D. J., J. M. Cregg, W. A. J. Dunn, Jr., S. D. Emr, Y. Sakai, I. V. Sandoval, A. Sibirny, S. Subramani, M. Thumm, M. Veenhuis, and Y. Ohsumi.** 2003. A unified nomenclature for yeast autophagy-related genes. Dev. Cell **5:**539–545.
37. **Klionsky, D. J., and S. D. Emr.** 2000. Autophagy as a regulated pathway of cellular degradation. Science **290:**1717–1721.
38. **Kroemer, G., and J. C. Reed.** 2000. Mitochondrial control of cell death. Nat. Med. **6:**513–519.
39. **Larsen, K. E., E. A. Fon, T. G. Hastings, R. H. Edwards, and D. Sulzer.** 2002. Methamphetamine-induced degeneration of dopaminergic neurons involves autophagy and upregulation of dopamine synthesis. J. Neurosci. **22:**8951–8960.
40. **Lassus, P., X. Opitz-Araya, and Y. Lazebnik.** 2002. Requirement for caspase-2 in stress-induced apoptosis before mitochondrial permeabilization. Science **297:**1352–1354.
41. **Lee, C. Y., E. A. Clough, P. Yellon, T. M. Teslovich, D. A. Stephan, and E. H. Baehrecke.** 2003. Genome-wide analyses of steroid- and radiation-triggered programmed cell death in *Drosophila*. Curr. Biol. **13:**350–357.
42. **Leist, M., and M. Jaattela.** 2001. Four deaths and a funeral: from caspases to alternative mechanisms. Nat. Rev. Mol. Cell Biol. **2:**589–598.
43. **Lemasters, J. J., A.-L. Nieminen, T. Qian, L. C. Trost, S. P. Elmore, Y. Nishimura, R. A. Crowe, W. E. Cascio, C. A. Bradham, D. A. Brenner, and B. Herman.** 1998. The mitochondrial permeability transition in cell death: a common mechanism in necrosis, apoptosis and autophagy. Biochim. Biophys. Acta **1366:**177–196.
44. **Leverkus, M., M. R. Sprick, T. Wachter, T. Mengling, B. Baumann, E. Serfling, E.-B. Bröcker, M. Goebeler, M. Neumann, and H. Walczak.** 2003.

Proteasome inhibition results in TRAIL sensitization of primary keratinocytes by removing the resistance-mediating block of effector caspase maturation. Mol. Cell. Biol. **23:**777–790.
45. **Liang, X. H., S. Jackson, M. Seaman, K. Brown, B. Kempkes, H. Hibshoosh, and B. Levine.** 1999. Induction of autophagy and inhibition of tumorigenesis by beclin 1. Nature **402:**672–676.
46. **Liang, X. H., L. K. Kleeman, H. H. Jiang, G. Gordon, J. E. Goldman, G. Berry, B. Herman, and B. Levine.** 1998. Protection against fatal Sindbis virus encephalitis by beclin, a novel Bcl-2-interacting protein. J. Virol. **72:**8586–8596.
47. **Lockshin, R. A., and Z. Zakeri.** 2002. Caspase-independent cell deaths. Curr. Opin. Cell Biol. **14:**727–733.
48. **Martin, D. N., and E. H. Baehrecke.** 2004. Caspases function in autophagic programmed cell death in *Drosophila*. Development **131:**275–284.
49. **Martinez, I., S. Chakrabarti, T. Hellevik, J. Morehead, K. Fowler, and N. W. Andrews.** 2000. Synaptotagmin VII regulates Ca(2+)-dependent exocytosis of lysosomes in fibroblasts. J. Cell Biol. **148:**1141–1149.
50. **Mitsiades, N., C. S. Mitsiades, V. Poulaki, D. Chauhan, G. Fanourakis, X. Gu, C. Bailey, M. Joseph, T. A. Libermann, S. P. Treon, N. C. Munshi, P. G. Richardson, T. Hideshima, and K. C. Anderson.** 2002. Molecular sequelae of proteasome inhibition in human multiple myeloma cells. Proc. Natl. Acad. Sci. USA **99:**14374–14379.
51. **Mizushima, N., A. Yamamoto, M. Hatano, Y. Kobayashi, Y. Kabeya, K. Suzuki, T. Tokuhisa, Y. Ohsumi, and T. Yoshimori.** 2001. Dissection of autophagosome formation using Apg5-deficient mouse embryonic stem cells. J. Cell Biol. **152:**657–668.
52. **Nakagawa, T., H. Zhu, N. Morishima, E. Li, J. Xu, B. A. Yankner, and J. Yuan.** 2000. Caspase-12 mediates endoplasmic-reticulum-specific apoptosis and cytotoxicity by amyloid-beta. Nature **403:**98–103.
53. **Nemoto, T., I. Tanida, E. Tanida-Miyake, N. Minematsu-Ikeguchi, M. Yokota, M. Ohsumi, T. Ueno, and E. Kominami.** 2003. The mouse APG10 homologue, an authentic E2-like enzyme for Apg12p conjugation, facilitates MAP-LC3 modification. J. Biol. Chem. **278:**39517–39526.
54. **Ogier-Denis, E., J. J. Houri, C. Bauvy, and P. Codogno.** 1996. Guanine nucleotide exchange on heterotrimeric Gi3 protein controls autophagic sequestration in HT-29 cells. J. Biol. Chem. **271:**28593–28600.
55. **Opipari, A. W. J., L. Tan, A. E. Boitano, D. R. Sorenson, A. Aurora, and J. R. Liu.** 2004. Resveratrol-induced autophagocytosis in ovarian cancer cells. Cancer Res. **64:**696–703.
56. **Paglin, S., T. Hollister, T. Delohery, N. Hackett, M. McMahill, E. Sphicas, D. Domingo, and J. Yahalom.** 2001. A novel response of cancer cells to radiation involves autophagy and formation of acidic vesicles. Cancer Res. **61:**439–444.
57. **Patterson, G. H., and J. Lippincott-Schwartz.** 2002. A photoactivatable GFP for selective photolabeling of proteins and cells. Science **297:**1873–1877.
58. **Pattingre, S., C. Bauvy, and P. Codogno.** 2003. Amino acids interfere with the ERK1/2-dependent control of macroautophagy by controlling the activation of Raf-1 in human colon cancer HT-29 cells. J. Biol. Chem. **278:**16667–16674.
59. **Plas, D. R., and C. B. Thompson.** 2002. Cell metabolism in the regulation of programmed cell death. Trends Endocrinol. Metab. **13:**75–78.
60. **Qu, X., J. Yu, G. Bhagat, N. Furuya, H. Hibshoosh, A. Troxel, J. Rosen, E. L. Eskelinen, N. Mizushima, Y. Ohsumi, G. Cattoretti, and B. Levine.** 2003. Promotion of tumorigenesis by heterozygous disruption of the beclin 1 autophagy gene. J. Clin. Investig. **112:**1809–1820.
61. **Reggiori, F., and D. J. Klionsky.** 2002. Autophagy in the eukaryotic cell. Eukaryot. Cell **1:**11–21.
62. **Saeki, K., A. Yuo, E. Okuma, Y. Yazaki, S. A. Susin, G. Kroemer, and F. Takaku.** 2000. Bcl-2 down-regulation causes autophagy in a caspase-independent manner in human leukemic HL60 cells. Cell Death Differ. **7:**1263–1269.
63. **Seglen, P. O., and P. B. Gordon.** 1982. 3-Methyladenine: specific inhibitor of autophagic/lysosomal protein degradation in isolated rat hepatocytes. Proc. Natl. Acad. Sci. USA **79:**1889–1892.
64. **Sullivan, P. G., N. B. Dragicevic, J. H. Deng, Y. Bai, E. Dimayuga, Q. Ding, Q. Chen, A. J. Bruce-Keller, and J. N. Keller.** 2004. Proteasome inhibition alters neural mitochondrial homeostasis and mitochondria turnover. J. Biol. Chem. **279:**20699–20707.
65. **Tanaka, Y., G. Guhde, A. Suter, E. L. Eskelinen, D. Hartmann, R. Lullmann-Rauch, P. M. Janssen, J. Blanz, K. von Figura, and P. Saftig.** 2000. Accumulation of autophagic vacuoles and cardiomyopathy in LAMP-2-deficient mice. Nature **406:**902–906.
66. **Tsukada, M., and Y. Ohsumi.** 1993. Isolation and characterization of autophagy-defective mutants of *Saccharomyces cerevisiae*. FEBS Lett. **333:**169–174.
67. **Voorhees, P. M., E. C. Dees, B. O'Neil, and R. Z. Orlowski.** 2003. The proteasome as a target for cancer therapy. Clin. Cancer Res. **9:**6316–6325.
68. **Wang, X.** 2002. The expanding role of mitochondria in apoptosis. Genes Dev. **15:**2922–2933.
69. **Wei, M. C., W.-X. Zong, E. H.-Y. Cheng, T. Lindsten, V. Panoutsakopoulou, A. J. Ross, K. A. Roth, G. R. MacGregor, C. B. Thompson, and S. J. Korsmeyer.** 2001. Proapoptotic BAX and BAK: a requisite gateway to mitochondrial dysfunction and death. Science **292:**727–730.
70. **Xue, L., G. C. Fletcher, and A. M. Tolkovsky.** 2001. Mitochondria are selectively eliminated from eukaryotic cells after blockade of caspases during apoptosis. Curr. Biol. **6:**361–365.
71. **Yamamoto, A., Y. Tagawa, T. Yoshimori, Y. Moriyama, R. Masaki, and Y. Tashiro.** 1998. Bafilomycin A1 prevents maturation of autophagic vacuoles by inhibiting fusion between autophagosomes and lysosomes in rat hepatoma cell line, H-4-II-E cells. Cell Struct. Funct. **23:**33–42.
72. **Yanagisawa, H., T. Miyashita, Y. Nakano, and D. Yamamoto.** 2003. HSpin1, a transmembrane protein interacting with Bcl-2/Bcl-xL, induces a caspase-independent autophagic cell death. Cell Death Differ. **10:**798–807.
73. **Yoshimori, T.** 2004. Autophagy: a regulated bulk degradation process inside cells. Biochem. Biophys. Res. Commun. **313:**453–458.
74. **Yoshimori, T., A. Yamamoto, Y. Moriyama, M. Futai, and Y. Tashiro.** 1991. Bafilomycin A1, a specific inhibitor of vacuolar-type H(+)-ATPase, inhibits acidification and protein degradation in lysosomes of cultured cells. J. Biol. Chem. **266:**17707–17712.
75. **Yue, Z., A. Horton, M. Bravin, P. L. DeJager, F. Selimi, and N. Heintz.** 2002. A novel protein complex linking the δ2 glutamate receptor and autophagy: implications for neurodegeneration in lurcher mice. Neuron **35:**921–933.
76. **Yue, Z., S. Jin, C. Yang, A. J. Levine, and N. Heintz.** 2003. Beclin 1, an autophagy gene essential for early embryonic development, is a haploinsufficient tumor suppressor. Proc. Natl. Acad. Sci. USA **100:**15077–15082.
77. **Zamzami, N., D. Métivier, and G. Kroemer.** 2000. Quantitation of the mitochondrial transmembrane potential in cells and in isolated mitochondria. Methods Enzymol. **322:**208–213.